



Cite this: *Catal. Sci. Technol.*, 2022, 12, 3356

Continuous flow for enantioselective cyanohydrin synthesis†

Dominika Stradomska, ^a José Coloma, ^{bc}
Ulf Hanefeld ^{*b} and Katarzyna Szymańska ^{*a}

Enantiomerically pure cyanohydrins are of great importance in the chemical and pharmaceutical industries. Their synthesis is possible through the use of highly selective hydroxynitrile lyases. In this work, an *R*-selective hydroxynitrile lyase (*AtHNL*) from *Arabidopsis thaliana* was immobilized inside a silica microreactor with a tortuous and hierarchical pore structure. After immobilization, the enzyme activity was tested for benzaldehyde **1a**, and its analogs 4-fluorobenzaldehyde **1b**, 4-methoxybenzaldehyde **1c** and 4-(trifluoromethyl)benzaldehyde **1d**. With their different degrees of reactivity they also display a different susceptibility to the racemic chemical background reaction. It was shown that the use of a flow microreactor suppressed the background reaction even for the most susceptible substrate **1d**. Furthermore, the use of a flow microreactor enabled high substrate conversion (90–95%) while maintaining a high enantiomeric excess (90–98%) with residence times of 3 to 30 min. The productivity, which depended on substrate reactivity and flow rate, was evaluated by space-time-yield (STY) and reached a value from 60 g L⁻¹ h⁻¹ to 1290 g L⁻¹ h⁻¹. Additionally it was demonstrated that the stability of the immobilized enzyme depends on the flow rates used and thus on the shear forces acting inside the microreactor and interfacial effects associated with them.

Received 11th January 2022,
Accepted 13th April 2022

DOI: 10.1039/d2cy00054g

rsc.li/catalysis

Introduction

The enantioselective synthesis of cyanohydrins is today performed by biocatalysis.^{1,2} The hydroxynitrile lyases (HNL) are highly efficient catalysts that enable the formation of both *S*- and *R*-cyanohydrins.³ Several industrial scale syntheses with these enzymes have been realized in a batch mode, utilizing *Hevea brasiliensis* HNL (*HbHNL*) or *Prunus amygdalus* HNL (*PaHNL*).^{3,4} In recent years it was demonstrated that these enzymes can be immobilized.^{3,5–10} The immobilized HNLs can be used in wet organic solvents and recycled many times. More importantly this allowed switching from batch to flow reactors. For several HNLs it was demonstrated that continuous flow reactors (CFR) gave much higher space-time yields (STY) than batch reactions as well as improved enantioselectivity.^{7–10} This last point is essential as the bottle-

neck in enantioselective cyanohydrin catalysis is the competing racemic chemical background reaction.^{1,3} This reaction is typically suppressed by utilizing pH values around 5, employing organic solvents and reducing the reaction time.^{1,8,11–13} CFRs add an additional tool to achieve this target.^{8–10}

In a detailed analysis of the *S*-selective *HbHNL* and *Manihot esculenta* HNL (*MeHNL*) it could be demonstrated that these two structurally closely related HNLs were readily immobilized on siliceous carriers and loaded onto monolithic CFR.⁸ Comparison between batch and flow revealed a huge improvement of STY (STY in flow 54 and 71 g L⁻¹ h⁻¹ mg_{protein}⁻¹ for *HbHNL* and *MeHNL* respectively rather than 30 h for 90% conv. in batch, STY ~1 g L⁻¹ h⁻¹ mg_{protein}⁻¹) and enantioselectivity (batch ~40% ee at 90% conv., flow continuously >95% ee at >95% conv.).

The *S*-selective *HbHNL* and *MeHNL* both have an α/β -hydrolase fold.^{1,11,14} Similarly *Arabidopsis thaliana* HNL (*AtHNL*) has this fold, however it is *R*-selective.^{11,14,15} It is special among the *R*-selective HNLs as it is the only one with an α/β hydrolase fold and its displays great synthetic versatility.^{1–3,7,15} *AtHNL* has been immobilized on Celite and applied in batch and flow with modest STY.⁷ When immobilized via a His₆-tag on EziG Opal STY of up to 690 mol_{product} h⁻¹ L⁻¹ genzyme⁻¹ could be achieved in flow, however the enantioselectivity decreased soon.⁹ Here we describe the

^a Department of Chemical Engineering and Process Design, Silesian University of Technology, Ks. M. Strzody 7, 44-100 Gliwice, Poland.

E-mail: Katarzyna.Szymanska@polsl.pl

^b Department of Biotechnology, Section Biocatalysis, Delft University of Technology, Van der Maasweg 9, 2629 HZ Delft, The Netherlands.

E-mail: U.Hanefeld@tudelft.nl

^c Universidad Laica Eloy Alfaro de Manabí, Avenida Circunvalación s/n, P.O. Box 13-05-2732, Manta, Ecuador

† Electronic supplementary information (ESI) available. See DOI: <https://doi.org/10.1039/d2cy00054g>



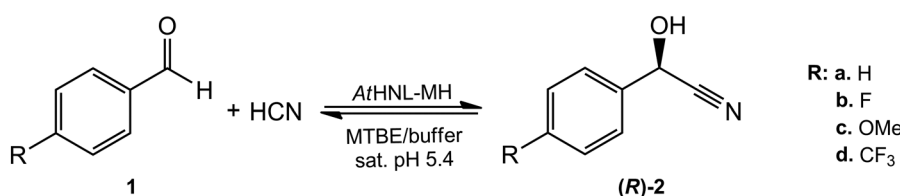
immobilization of this *R*-selective *AtHNL* on a siliceous monolith microreactor and its application in CFRs, in line with the earlier studies with *MeHNL* and *HbHNL*,⁸ where it has been demonstrated that the use of CFRs allows virtual elimination of the background reaction, enabling high substrate conversion while maintaining very good process selectivity. Achieving such results was not possible with the use of particles of immobilised catalysts in a batch reactor.⁸ For the above reasons, in this work we will focus on processes carried out in flow microreactors. To rigorously probe whether the racemic chemical background reaction is fully suppressed and the desired improvement of enantioselectivity is achieved very reactive aldehydes (benzaldehyde **1a**, and its analogs: 4-fluorobenzaldehyde **1b**, 4-methoxybenzaldehyde **1c** and 4-(trifluoromethyl)-benzaldehyde **1d**, Scheme 1) are utilized. These aldehydes are particularly susceptible to the racemic chemical background reaction and only with a very efficient reaction system can high enantioselectivity be achieved.

Results and discussion

In this study we evaluate the performance of covalently immobilized *AtHNL* in a siliceous monolithic microreactor for the synthesis of (*R*)-cyanohydrins in a continuous flow system. Synthesis reactions in standard batch systems often require long reaction times and strong stirring to avoid diffusion limitation resulting in low output and mechanical attrition of the heterogeneous catalyst.¹⁶ All these limitations can be circumvented by using continuous flow processes and reactors. The continuous mode allows for waste reduction, process intensification, and ease of catalyst reusability without separation.¹⁷ Moreover, the small volumes of microreactors enable better control of reaction parameters, higher outputs, and safer processes.¹⁸ These methods are in line with the current 'green chemistry' trends.^{17,19–21} In this work we have applied hierarchically structured silica monoliths with tortuous pore structure and high surface-to-volume ratio ($4 \times 10^7 \text{ m}^2 \text{ m}^{-3}$), which allows for intensive homogenization of reactants and enhanced mass transport of substrates to the active center of the enzyme. Additionally, silica carriers exhibit very good stability in organic solvents.^{8,22} The (*R*)-selective HNL from *Arabidopsis thaliana* (*AtHNL*) was immobilized inside amino modified silica monoliths (1.3 mmol of amino groups per 1 g of silica – measured by elemental analysis), the amino groups were

activated by glutaraldehyde. Glutaraldehyde tends to self-polymerize, forming a branched structure and thus generating more sites for enzyme immobilization.²³ This enzyme is a dimer and displays a largely hydrophilic surface with 19 lysine residues per monomer; *i.e.* 0.605 mmol per g of enzyme (Fig. 1). Therefore, an amino functionalized silica carrier is a suitable material for its immobilization. Typically, immobilized HNLs are effectively used in monophasic systems of buffer saturated organic solvents such as methyl *tert*-butyl ether (MTBE) or diisopropyl ether as the reaction medium. To overcome the non-selective chemical background reaction, the methyl *tert*-butyl ether was saturated with citrate/phosphate buffer pH 5.4, as the native *AtHNL* has a pH optimum between 5.75 and 6.5, but it is also almost inactive below pH 5.0 unless immobilized (Scheme 1).

To establish a base line the undesired racemic background reaction was investigated first. The susceptibility of the substrates to this reaction catalyzed by the siliceous carriers functionalized with amino groups and activated with glutaraldehyde was therefore determined (Fig. 2). The electron rich substrate **1c** is the least susceptible to the racemic background reaction, as it is the least reactive. Even with half an hour residence time only 3.5% conversion was observed. The obtained results suggest that in case of this substrate, a racemic background reaction does not threaten the enantiomeric purity of the obtained final product. For substrates **1a** and **1b** a similar susceptibility to the background reactions was observed. It was, however, 5 times higher than for substrate **1c**. The substrate conversion level ranged from 13% to 15% with a residence time of 25–30 min. Substrate **1d** was very susceptible to the racemic background reaction. In this case, the conversion was approx. 35% with a residence time of about 30 minutes and decreased only three folds with a 10-fold reduction in the residence time. The latter results suggest that for **1d** it will be very difficult to obtain the final product with a satisfactory optical purity; it thus is an ideal probe for the scope of our approach. The immobilization of *AtHNL* in microreactors proceeded *via* amine functionalized silica monoliths activated with glutaraldehyde, as described earlier for the structurally related *MeHNL* and *HbHNL*.⁸ The number of amino groups on the carrier and thus the glutaraldehyde available significantly outnumbered the amino groups on the *AtHNL* surface. The immobilization was performed at ambient temperatures with equal amounts of enzyme. Three microreactors bound a similar amount of protein (10–13 mg),



Scheme 1 Enantioselective synthesis of (*R*)-cyanohydrins (*R*)-2 from aromatic aldehydes (**1a–d**) and hydrogen cyanide catalyzed by immobilized *AtHNL*.



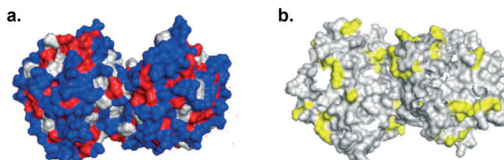


Fig. 1 Surface visualisation of dimeric AtHNL (PDB code: 3dqz): a. residues in blue (arg, lys, his, glu, asp, asn, gln, thr, ser, cys) are hydrophilic, residues in grey (pro, tyr, typ) have intermediate polarity and residues in red (ala, gly, val, ile, leu, phe, met) are hydrophobic; b. residues in yellow are lysines. The images were created using PyMOL molecular graphics system.

while one batch of enzyme gave better binding of about 20 mg (20–22 mg). The difference in loading might possibly be due to temperature fluctuations (2–4 °C) during immobilization or conceivably due to the use of different enzyme batches and slight differences in protein purity.

As substrates **1a**, **1b** and **1c** are less challenging the reactor with 10–13 mg of AtHNL were used for them and the reactor with 20 mg of AtHNL was employed for the most challenging substrate **1d** (Fig. 3). As expected, the lowest activity and space-time-yield (STY) was exhibited by **1c** (STY in the range 60–210 g L⁻¹ h⁻¹, depending on flow rate). However, even for this substrate, using appropriately long residence times (approx. 30 min), it was possible to achieve 90% conversion while maintaining over 90% enantiomeric

excess. A similar conversion, with the use of the same enzyme and substrate, was achieved in the work of Andexer *et al.*¹⁵ although the process time was 22 h and the enantiomeric excess 68%. Slightly better results were obtained in the works of Koch *et al.*²⁴ and Nanda *et al.*²⁵ (conversion at the level of 50% and 17%, respectively, enantiomeric excess approx. 97%, process time 30 min), with the use of HNL isolated from *Hevea brasiliensis* and *Prunus mume*.

1a and **1b** showed similar reactivity and STY (STY(**1a**) = 70–440 g L⁻¹ h⁻¹, STY(**1b**) = 70–670 g L⁻¹ h⁻¹). With residence times greater than 5 min, practically 100% substrate was converted with over 95% enantiomeric excess. Previously, similar values were obtained only when employing significantly longer residence times.^{5,6,15,25,26} The key test was substrate **1d**. Due to its high reactivity favouring an unselective background reaction (Fig. 2d), there were concerns as to whether it would be possible to obtain a product with a satisfactory enantiomeric excess. However, also in this case, the use of a flow microreactor allowed to obtain the final product not only with a very high conversion (90–100%), but more importantly, with a very good enantiomeric excess (above 95%), with residence times above 4 min. Importantly, for this substrate (**1d**) a remarkable space-time-yield was obtained (120–1290 g L⁻¹ h⁻¹). The target of establishing a system that can convert even demanding substrates with high enantiomeric excesses has

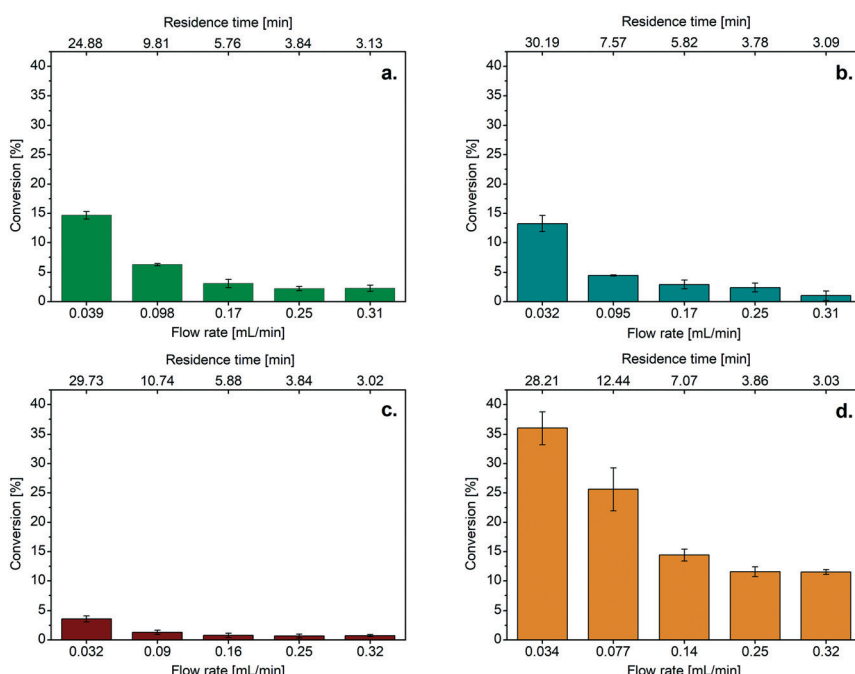


Fig. 2 Background reaction (glutaraldehyde activated monolith without enzyme, 4 cm, ø 6 mm): a. benzaldehyde **1a** on stream with linear flow velocity 0.14–1.10 cm min⁻¹, b. 4-fluorobenzaldehyde **1b** on stream with linear flow velocity 0.11–1.10 cm min⁻¹, c. 4-methoxybenzaldehyde **1c** on stream with linear flow velocity 0.11–1.13 cm min⁻¹, d. 4-(trifluoromethyl)benzaldehyde **1d** on stream with linear flow velocity 0.12–1.13 cm min⁻¹, conversion (bars) vs. flow rate (mL min⁻¹)/residence time (min). Conditions: aldehyde 0.25 M, 1,3,5-triisopropylbenzene (ISTD) 0.033 M for benzaldehyde, 4-fluorobenzaldehyde and 4-(trifluoromethyl)benzaldehyde and 0.1 M for 4-methoxybenzaldehyde, HCN 0.75–1.0 M in MTBE saturated with citrate/phosphate buffer (pH 5.4, 50 mM), room temperature (~20 °C). Error bars indicate the standard deviation based on triplicate HPLC samples.



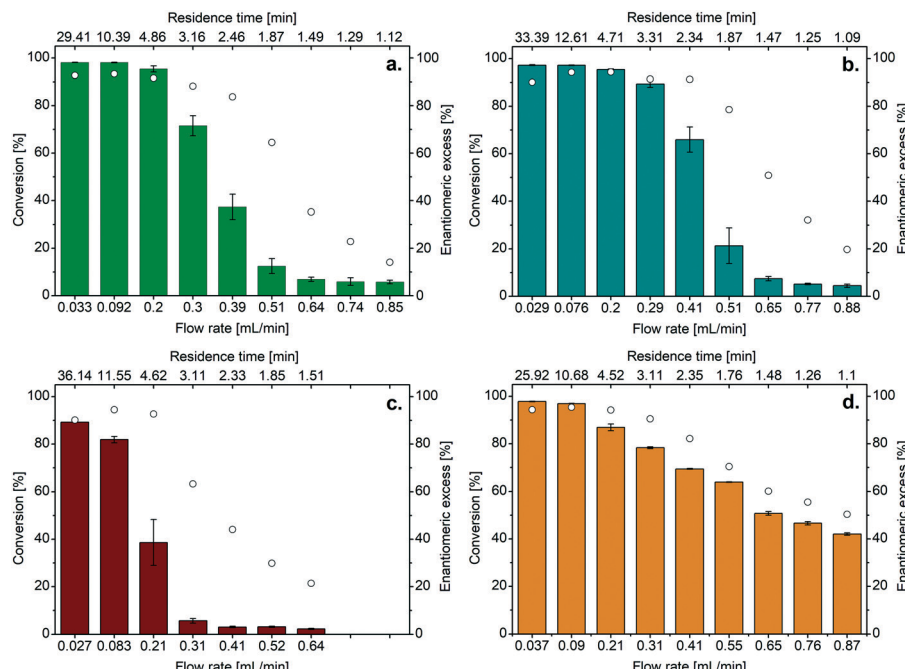


Fig. 3 Synthesis of (R)-cyanohydrins: a. benzaldehyde **1a**, AtHNL-MH (10.8 mg total protein, 1469 U per monolith, 4 cm, ϕ 6 mm) on stream with linear flow velocity 0.12–3.00 cm min^{-1} , b. 4-fluorobenzaldehyde **1b**, AtHNL-MH (10.2 mg total protein, 1387 U per monolith, 4 cm, ϕ 6 mm) on stream with linear flow velocity 0.10–3.11 cm min^{-1} , c. 4-methoxybenzaldehyde **1c**, AtHNL-MH (13.5 mg total protein, 1836 U per monolith, 4 cm, ϕ 6 mm) on stream with linear flow velocity 0.10–2.26 cm min^{-1} , d. 4-(trifluoromethyl)benzaldehyde **1d**, AtHNL-MH (20.6 mg total protein, 2802 U per monolith, 4 cm, ϕ 6 mm) on stream with linear flow velocity 0.13–3.07 cm min^{-1} , conversion (bars)/enantiomeric excess (spots) vs. flow rate (mL min^{-1})/residence time (min). Conditions: aldehyde 0.25 M, 1,3,5-triisopropylbenzene (ISTD) 0.033 M for benzaldehyde, 4-fluorobenzaldehyde and 4-(trifluoromethyl)benzaldehyde and 0.1 M for 4-methoxybenzaldehyde, HCN 0.75–1.0 M in MTBE saturated with citrate/phosphate buffer (pH 5.4, 50 mM), room temperature ($\sim 20^\circ\text{C}$). Error bars indicate the standard deviation based on triplicate HPLC samples.

thus been met. For all four tested substrates, an increased flow rate and thus decreased residence time led to decreased conversions and enantioselectivities.

This decrease in enantiomeric excess with increasing flow rate is unexpected.⁸ It may suggest either the leaching of the enzyme from the microreactor or its deactivation as a result of the shear forces and interfacial effects associated with them and with the flow of reagents through the microreactor

macropores. Therefore we probed the microreactor stability using two substantially different flow rates, and thus two different linear flow velocities and different shear forces (Fig. 4). Employing flow rates of 0.5 and 0.1 mL min^{-1} with microreactor diameters of 6 mm and 4 mm, respectively, yields linear velocities of 1.7 and 0.75 cm min^{-1} . The obtained results clearly indicate that the use of higher flow rates causes a faster decrease in activity. The use of a flow rate of

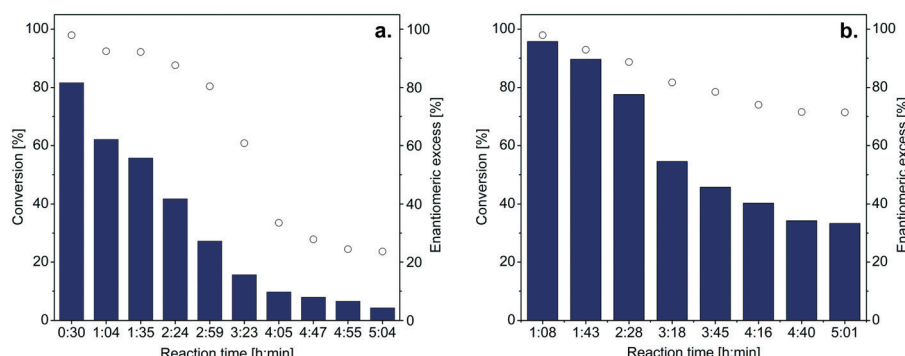


Fig. 4 Stability of AtHNL-MH for (R)-mandelonitrile synthesis reaction: a. 2.7 cm piece (ϕ 6 mm) of AtHNL-MH (25.8 mg total protein, 3509 U per monolith) on stream with flow rate 0.49 mL min^{-1} (linear flow velocity 1.73 cm min^{-1}), b. 3.0 cm piece (ϕ 4 mm) of AtHNL-MH (5.4 mg total protein, 734 U per monolith) on stream with flow rate 0.094 mL min^{-1} (linear flow velocity 0.75 cm min^{-1}), conversion (bars)/enantiomeric excess (spots) vs. reaction time (h:min). Conditions: benzaldehyde **1a** 0.25 M, 1,3,5-triisopropylbenzene (ISTD) 0.033 M, HCN 0.75–1.0 M in MTBE saturated with citrate/phosphate buffer (pH 5.4, 50 mM), room temperature ($\sim 20^\circ\text{C}$).

0.5 mL min^{-1} resulted in a 50% decrease in activity after 2.24 hours, while the same effect for a flow rate of 0.1 mL min^{-1} occurred only after about 4 hours. Before and after the stability tests, the microreactor was subjected to an infrared spectrometric analysis to verify whether the enzyme had leached. The IR analysis of microreactors taken before and after the reaction indicated the presence of C–N stretching vibration (1480–1570 cm^{-1}) characteristic for peptide bonds (Fig. 5). These vibrations were not observed for amino functionalized and glutaraldehyde activated monolithic microreactors. The strong band proves that the enzyme is still in the reactor volume. The decrease in activity is hence most likely due to damage to the protein structure caused by the flow of reagents and the associated shear forces. The drastic conditions leading to deactivation are however not necessary to obtain the highest conversions and enantioselectivities (Fig. 3). These were obtained at flow rates equal to about 0.03 mL min^{-1} (linear flow velocity about 0.1 cm min^{-1}), the shear forces generated by these flows should not pose a significant threat to the stability of the enzyme under the desired conditions.

Conclusions

The *R*-selective hydroxynitrile lyase from *Arabidopsis thaliana* (*AtHNL*) was immobilized inside monolithic flow microreactors and its activity was then studied in the presence of benzaldehyde derivatives. These derivatives exhibited different reactivity and thus different susceptibility to the non-selective chemical background reaction. It was shown that the use of microreactors with a unique meandering pore structure allowed for simultaneous high degree of substrate conversion and enantiomeric excess even when using a reactive substrate such as **1d**. This demonstrates that this reactor concept can successfully suppress undesired side reactions to an extent otherwise not possible. Furthermore, the immobilized *AtHNL* was shown to

be stable under the desired reaction conditions. Shear forces only affected the enzyme at significantly higher flow rates, pointing to a further advantage of the monolithic flow microreactors.

Experimental

General

Unless otherwise stated, all chemicals were obtained in the highest available purity from commercial sources (Acros Organics, Fluka, J.T. Baker, Avantor Poland) and used without further purification. All aldehydes were stored under argon atmosphere. Benzaldehyde was distilled prior to use. 4-Fluorobenzaldehyde was stored at 4 °C. For the aqueous buffers preparation distilled water and analytical grade salts were utilized.

HPLC analysis were performed on Agilent Technologies 1200 series equipped with UV/vis, column thermostat, autosampler, HPLC pumps and a Daicel Chiralpak AD-H column (250 × 4.6 mm, 5 μm). Samples (8 μL for **1c** or 25 μL for **1a**, **1b**, **1d**) were diluted in 1 mL heptane/isopropanol (95 : 5), dried over anhydrous MgSO_4 and centrifuged, then 10 μL of the sample was injected into the HPLC system. The applied HPLC method settings were as follows: mobile phase: heptane : isopropanol 95 : 5, UV detection wavelength: $\lambda = 216$ nm, oven temperature: 40 °C, flow rate: 1 mL min^{-1} . The retention times of all substrates and products are given in ESI.†

Synthesis of silica monolith and their functionalization

Amino functionalized silica monoliths with hierarchical pore structure were obtained according method described in Szymańska *et al.*²⁷ and van der Helm *et al.*⁸ Briefly, polyethylene glycol 35 000 was dissolved in 1 M HNO_3 and then tetraethoxysilane (TEOS) and cetyltrimethylammonium bromide (CTAB) were added. The received alcogels were impregnated with 1 M ammonia water solution and subsequently dried and calcinated. The monoliths were then functionalized with 3-aminopropyltrimethoxysilane in dry toluene and clad with polymer resin to obtain single-rod microreactors. Details of the procedure are given in ESI.†

Production and purification of *Arabidopsis thaliana* HNL (*AtHNL*)

Arabidopsis thaliana HNL (*AtHNL*) was heterologous expressed and subsequently purified according to Coloma *et al.*⁹ The pET28a-*AtHNL* expression plasmid containing the *AtHNL* gene (GenBank accession number AAN13041, EC:4.1.2.10) codon optimized for *E. coli* and with a polyhistidine tag (His₆-tag) was obtained from the group of Prof. Dr. Martina Pohl (Institute of Bio- and Geosciences, Jülich, Germany). Details of the procedure are given in ESI.†

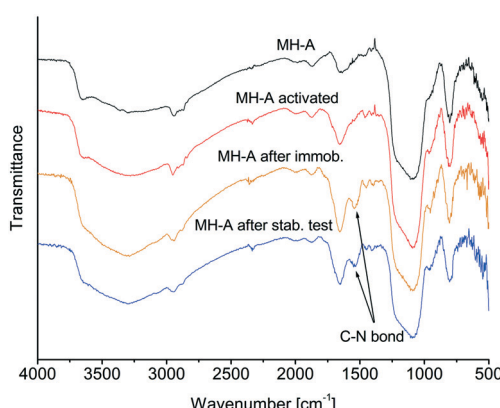


Fig. 5 FTIR spectra of silica monoliths functionalized with amino groups (black) and subsequently activated by glutaraldehyde (red). Orange and blue line are for *AtHNL* immobilized on silica monolith respectively just after immobilization (orange) and after stability test (blue).



Enzyme immobilization on the silica monolith

Before the attachment of *AtHNL* amino-functionalized monolith (6 × 40 mm) was washed with ethanol and distilled water for 80 min each (45 mL h⁻¹) and then by phosphate buffer (Na₂HPO₄/KH₂PO₄, 100 mM, pH 7.0) for 40 min (45 mL h⁻¹). For activation of the amino groups 2.5% (v/v) glutaraldehyde solution (in phosphate buffer, 100 mM, pH 7.0) was pumped for 90 min (60 mL h⁻¹), followed by distilled water for 90 min (60 mL h⁻¹) and phosphate buffer (100 mM, pH 7.0) for another 70 min (45 mL h⁻¹) to wash off the glutaraldehyde excess. 5.0 mL of the protein solution in phosphate buffer (100 mM, pH 7.0) was circulated through the microreactor for 90 min (20 mL h⁻¹) at room temperature and suspended overnight at 4 °C. The excess of protein was removed by phosphate buffer (100 mM, pH 7.0) washing for 40 min (3 mL h⁻¹) and additional 30 min (5 mL h⁻¹), then 500 mM NaCl solution in phosphate buffer (100 mM, pH 7.0) for 60 min (30 mL h⁻¹), sodium acetate buffer (100 mM, pH 4.5) for 30 min (30 mL h⁻¹) and distilled water for 60 min (30 mL h⁻¹). Finally, microreactor with immobilized enzyme was washed with TRIS-HCl buffer (500 mM, pH 8.0) for 15 min (30 mL h⁻¹) and suspended overnight at 4 °C. Eluates from the immobilization steps were collected and using the Lowry Assay the amount of immobilized protein was determined using UV/vis spectrometer Hitachi U-2800A. As a standard a bovine serum albumin (BSA) calibration curve was used.

Preparation of HCN solution in MTBE

HCN solution in MTBE was obtained according to method described by van der Helm *et al.*⁸ and Coloma *et al.*⁹ Before synthesis MTBE and distilled water were cooled down at 0 °C. Potassium or sodium cyanide (6.51 or 4.9 g respectively, 0.1 mol) was dissolved in water (10 mL) and MTBE (25 mL), and magnetically stirred for 15 min in an ice bath. To the biphasic system 30% (v/v) aqueous HCl (10 mL) was added dropwise and the obtained HCN solution was allowed to reach room temperature (about 25 min). The organic phase was then separated from the aqueous one and collected. The separation was repeated twice more by adding MTBE (7 mL) each time. The final HCN solution (1.5–2.0 M) was kept over citrate/phosphate buffer (50 mM, pH 5.4) in a 1:1 ratio and stored in a dark bottle at 4 °C.

Caution: potassium cyanide (KCN) and hydrogen cyanide (HCN) are highly poisonous chemicals. All experiments involving KCN and HCN were performed in a ventilated fume hood with 2 calibrated HCN detectors (inside and outside the fume hood). HCN wastes were neutralized over a large excess of commercial bleach (15% sodium hypochlorite solution) for disposal.

Synthesis of (*R*)-mandelonitriles 2a–d

Before starting the reaction, the monolith with immobilized *AtHNL* was rinsed with water for 30 min (30 mL h⁻¹) and citrate/phosphate buffer (50 mM, pH 5.4) for 30 min (15 mL h⁻¹). The previously prepared substrates: 0.5 M aldehyde

(with 0.066 M (**1a**, **1b**, **1d**) or 0.2 M (**1c**) 1,3,5-triisopropylbenzene ISTD) solution in MTBE and 1.5–2.0 M HCN solution in MTBE saturated with citrate/phosphate buffer (50 mM, pH 5.4) were mixed in a 1:1 (v/v) ratio and then pumped through the monolith by infusion pump (Legato100) equipped with glass syringe. To initiate the reactions, the set flow rate was stabilized for an appropriate time and then three samples for each flow rate were collected. Every single sample was weighted to check the flow rate (flow rate = (weight of sample/density)/time). Concentrations of substrates and products' enantiomeric excess at different flow rate were determined with chiral HPLC.

Stability studies for different flow rate

Testing of the stability was performed for *AtHNL*-MH (6 × 30 mm, 25.8 mg total protein, 3509 U) and *AtHNL*-MH (4 × 27 mm, 5.4 mg total protein, 734 U), which were left for prolonged time on stream at respectively 0.49 mL min⁻¹ flow rate (linear speed 1.73 cm min⁻¹) and 0.094 mL min⁻¹ flow rate (linear speed 0.75 cm min⁻¹). Samples were taken at regular intervals and analyzed by chiral HPLC.

Author contributions

DS: conceptualization, investigation, visualization, writing – original draft, JC: conceptualization, investigation, visualization, writing – original draft, UH: conceptualization, supervision, writing – review & editing, KS: conceptualization, supervision, writing – review & editing.

Conflicts of interest

There are no conflicts to declare.

Acknowledgements

This project is financed by the National Science Centre of Poland (NCN) under grant UMO-2016/23/B/ST8/00627 and the Secretary of Higher Education, Science, Technology and Innovation of Ecuador and Universidad Laica Eloy Alfaro de Manabí (ULEAM). We thank Dr. Luuk Mestrom for stimulating discussions.

Notes and references

- 1 J. N. Andexer, J. V. Langermann, U. Kragl and M. Pohl, *Trends Biotechnol.*, 2009, **27**, 599–607.
- 2 P. Bracco, H. Busch, J. Von Langermann and U. Hanefeld, *Org. Biomol. Chem.*, 2016, **14**, 6375–6389.
- 3 U. Hanefeld, *Chem. Soc. Rev.*, 2013, **42**, 6308–6321.
- 4 E. Lanfranchi, K. Steiner, A. Glieder, I. Hajnal, R. A. Sheldon, S. van Pelt and M. Winkler, *Recent Pat. Biotechnol.*, 2013, **7**, 197–206.
- 5 D. Yildirim, S. S. Tükel and D. Alagöz, *Biotechnol. Prog.*, 2014, **30**, 818–827.
- 6 J. von Langermann and S. Wapenhensch, *Adv. Synth. Catal.*, 2014, **356**, 2989–2997.



7 A. Brahma, B. Musio, U. Ismayilova, N. Nikbin, S. B. Kamptmann, P. Siegert, G. E. Jeromin, S. V. Ley and M. Pohl, *Synlett*, 2016, **27**, 262–266.

8 M. P. van der Helm, P. Bracco, H. Busch, K. Szymańska, A. B. Jarzębski and U. Hanefeld, *Catal. Sci. Technol.*, 2019, **9**, 1189–1200.

9 J. Coloma, T. Lugtenburg, M. Afendi, M. Lazzarotto, P. Bracco, P.-L. Hagedoorn, L. Gardossi and U. Hanefeld, *Catalysts*, 2020, **10**, 899.

10 J. Coloma, Y. Guiavarc'h, P.-L. Hagedoorn and U. Hanefeld, *Catal. Sci. Technol.*, 2020, **10**, 3613–3621.

11 J.-K. Guterl, J. N. Andexer, T. Sehl, J. von Langermann, I. Frindi-Wosch, T. Rosenkranz, J. Fitter, K. Gruber, U. Kragl, T. Eggert and M. Pohl, *J. Biotechnol.*, 2009, **141**, 166–173.

12 M. Dadashipour and Y. Asano, *ACS Catal.*, 2011, **1**, 1121–1149.

13 B. Kopka, M. Diener, A. Wirtz, M. Pohl, K.-E. Jaeger and U. Krauss, *Biotechnol. J.*, 2015, **10**, 811–819.

14 J. N. Andexer, N. Staunig, T. Eggert, C. Kratky, M. Pohl and K. Gruber, *ChemBioChem*, 2012, **13**, 1932–1939.

15 J. Andexer, J. von Langermann, A. Mell, M. Bocola, U. Kragl, T. Eggert and M. Pohl, *Angew. Chem., Int. Ed.*, 2007, **46**, 8679–8681.

16 R. M. Lindeque and J. M. Woodley, *Catalysts*, 2019, **9**, 262.

17 L. Tamborini, P. Fernandes, F. Paradisi and F. Molinari, *Trends Biotechnol.*, 2018, **36**, 73–88.

18 M. Movsisyan, E. I. P. Delbeke, J. K. E. T. Berton, C. Battilocchio, S. V. Ley and C. V. Stevens, *Chem. Soc. Rev.*, 2016, **45**, 4892–4928.

19 C. Wiles and P. Watts, *Green Chem.*, 2012, **14**, 38–54.

20 K. F. Jensen, *AIChE J.*, 2017, **63**, 858–869.

21 J. Coloma, Y. Guiavarc'h, P.-L. Hagedoorn and U. Hanefeld, *Chem. Commun.*, 2021, **57**, 11416–11428.

22 D. Kowalczykiewicz, K. Szymańska, D. Gillner and A. B. Jarzębski, *Microporous Mesoporous Mater.*, 2021, **312**, 110789.

23 J.-K. Kim, J.-K. Park and H.-K. Kim, *Colloids Surf., A*, 2004, **241**, 113–117.

24 M. M. E. Delville, K. Koch, J. C. M. van Hest and F. P. J. T. Rutjes, *Org. Biomol. Chem.*, 2015, **13**, 1634–1638.

25 S. Nanda, Y. Kato and Y. Asano, *Tetrahedron*, 2005, **61**, 10908–10916.

26 S. Han, P. Chen, G. Lin, H. Huang and Z. Li, *Tetrahedron: Asymmetry*, 2001, **12**, 843–846.

27 K. Szymańska, W. Pudło, J. Mrowiec-Białoń, A. Czardybon, J. Kocurek and A. B. Jarzębski, *Microporous Mesoporous Mater.*, 2013, **170**, 75–82.

